

Mineralogy, Petrology and Chemistry of the Fotino Granitic Rocks, Thessaly, Central Greece.

ATHANASSIOS KATERINOPOULOS¹, ANDREAS KOKKINAKIS¹ and KONSTANTINOS KYRIAKOPOULOS¹

Section of Mineralogy and Petrology, Department of Geology, University of Athens, Panepistimiopolis, Ano Ilissia, GR-15784.

Abstract. The studied plutonic rocks are granites, presenting S-type characteristics. The mineral constituents have been studied by optical and chemical methods. The whole rock chemistry is studied in terms of major, trace and REE analyses. The petrography of the granites is described and the crystallisation sequence is discussed.

Major and trace elements show continuous smooth variation trends and REE patterns, with high LREE/HREE ratios, indicating a distribution strongly controlled by the fractionation of feldspars. The mantle normalised patterns show high LIL/HFS element ratios and negative Nb, Ti and P anomalies.

Fotino granites yielded muscovite ages ranging from 273 to 225 Ma, while the geochemical features suggest an increased crustal involvement to the composition of the parental magma. These magmas should have been generated in a subduction-related geotectonic environment, which has been active during the formation of the Hercynian fold belt.

Key words: Granite, Petrology, Geochemistry, Greece.

Introduction

The granitic intrusion in Fotino area was mapped by STAMATIS (1987). In this map a quartz monzonite body appears near Fotino village (Fig. 1), another one exists near Deskati village, while small occurrences of granite, granodiorite and quartz diorite are spread in the area.

KILIAS & MOUNTRAKIS (1989) studied the geotectonic evolution of the area on the basis of field relationship data. STAMATIS (1987) gave a short description of the petrographic types and a reference to their mineral constituents in the relative map.

For the purposes of this study, rock samples from the Fotino granitic rocks have been collected, studied for their petrography and analysed for their mineral chemistry and their major, trace and rare earth element composition. Petrogenetic features of the plutonic rocks are depicted from the correlation of the above data.

Geologic setting

The Fotino plutonic rocks intrude the Pieria-Kamvounia crystalline massif, a structural element of the

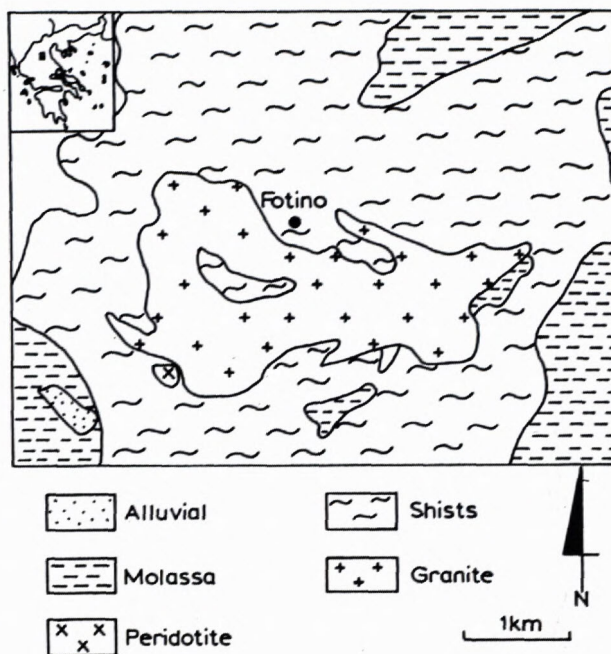


Fig. 1 Sketch map of the studied area

Pelagonian Nappe. According to KILIAS & MOUNTRAKIS (1989) the Pelagonian Nappe consists of:

- Limestones of Middle to Upper Cretaceous transgression and the Paleocene flysch.
- The western carbonate cover of Triassic to Jurassic age.
- The eastern carbonate cover of Triassic to Jurassic age.
- A metaclastic sequence of Late Permian - Early Triassic age.
- Three crystalline sequences (Vernon, Voras and Pieria-Kamvounia).
- Large granitic masses of different ages.

These crystalline sequences crystallised under similar conditions in the Paleozoic, but then they suffered different tectonic events as they present differences in their megastructure and their kinematics.

The Pieria-Kamvounia massif is characterised by a lower "Elassona" sequence, consisting of gneisses and amphibolites with migmatitic interpositions and an upper

Kefalovrysson" sequence consisting of schists with metabasite and marble intercalations.

According to KILIAS & MOUNTRAKIS (1989) the lithological and tectonic study indicates that the granites intruded the metamorphic rocks probably during Upper Jurassic-Lower Cretaceous.

In the Upper Cretaceous - Palaeocene the Pieria-Kamvounia crystalline massif overthrusts the blueschists of the Ambelakia unit and in Upper Eocene it is overthrust onto the carbonate masses of Olympos-Ossa, Rizomata and Krania carbonate sequences (MIGIROS 1983, KATSIKATSOS et al. 1986).

Sampling and analytical methods

Sampling was carried out with special care to collect unaltered samples from well preserved outcrops. The chemical analyses were made in the Department of Geology at the University of Leicester, England.

The mineral phases have been studied by polarised microscope and analysed by an automatic electron microprobe (JXA-8600 Superprobe) using the Energy Dispersive method. The standards used were of pure elements or natural compounds.

Major and trace element analyses were carried out by X-ray fluorescence method using a Philips PW 1400 series spectrometer. Details on the analytical procedure, precision and accuracy on the analytical techniques are given in MARSH et al (1983).

Rare earth elements were separated by chromatography and determined by inductive-couple plasma spectroscopy on an ICP Philips PW 8210 1.5 m.

Rb-Sr isotope analyses have been carried out at the Institute of Geochronology and Isotopic Geochemistry, CNR of Pisa, Italy, using a VG Isomass 54E mass spectrometer. The precision of the $^{87}\text{Rb}/^{86}\text{Sr}$ ratio determination has been estimated at $\pm 1\%$. The value of $1.42 \times 10^{-11} \text{ y}^{-1}$ was used for the ^{87}Rb decay constant. The mica ages were calculated adapting a $^{87}\text{Sr}/^{86}\text{Sr}$ correction of the corresponding whole rocks.

Mineralogy

a. Quartz: It is the most abundant mineral constituent, forming about 35 % of the studied samples. Primary quartz occurs in the form of irregular grains, as porphyroclasts or as aggregates consisting of randomly situated grains. Tectonism caused strong undulose extinction and biaxial optical character. Recrystallised quartz occurs in the form of small elongated grains, with irregular, interpenetrated edges, generally presenting a normal or a very weak undulose extinction.

b. Feldspars

b. 1. K-feldspar: Crosshatched microcline perthite is the dominant potassium feldspar forming about 35 % of the studied rocks. It is present in the form of porphyroclasts, or as allotropic interstitial grains. Almost all large microcline grains present the tartan twinning, while the smaller ones are usually twinning free.

Vein-perthites are very common. In all cases, perthites and host microcline grains have the same optical orientation. Albite inclusions are usual, while zircon, apatite and allanite inclusions are rare. Results of representative chemical analyses of K-feldspars and their structural formulae recalculated on the basis of 32 (O) are shown in Tables 1 and 2.

b. 2. Plagioclase: It is present in the form of stressed grains and fragments, or in aggregates composed of allotropic isodiametric porphyroclasts of albite or oligoclase. It is often replaced by K-feldspar and decomposed to quartz, sericite, epidote, titanite and garnet. Some of the chemical constituents of these secondary products result from the decomposition of neighbouring biotite crystals.

The larger grains present twinning according to the albite law and rarely to the pericline or karlsbad ones. Representative chemical analyses of Na-Ca-feldspars and their structural formulae recalculated on the basis of 22 (O) are listed in Tables 3 and 4.

b. 3. Inclusions: Both sodium and potassium feldspars are included in larger albite and microcline crystals. Chemical analyses of included feldspars and their structural formulae recalculated on the basis of 32 (O) are given in Table 5.

c. Micas

c. 1. Muscovite: It is present in all the studied samples, appearing in idiomorphic weakly pleochroic crystals, with an elongation ratio usually ranging from 2 to 4. In most cases it replaces biotite or plagioclase. This replacement of primary minerals by muscovite is usually developed parallel to the cleavage and twinning surfaces, or along cracks. The so formed fine sericite flakes are arranged parallel to the above mentioned surfaces.

Larger muscovite crystals bear on the outer surfaces, or along the cleavage and cracks, small isodiametric opaque mineral grains. Representative analyses of muscovite along with their structural formulae based on 22 [O] are shown in Table 6.

c. 2. Biotite: It occurs in small amounts, so it can be considered an accessory mineral in most cases. It usually appears as idiomorphic to hypidiomorphic flakes.

Most biotite crystals have been mechanically deformed so that the elongation ratio ranges from 10 to 20 and decomposed to sericite, epidote, titanite, magnetite, apatite and garnet, pseudomorphically developed. The decomposition of adjacent feldspar crystals provided the necessary Ca, Si, Al, and K for these phases.

The biotite flakes are iron enriched, so their colour is dark brownish-red parallel to (001) and brown perpendicular to (001). Results of representative chemical analyses of biotites and their structural formulae recalculated on the basis of 22 (O) are listed in Table 6.

d. Accessory minerals: Accessory phases include titanite, epidote, allanite, zircon, garnet, apatite and opaque minerals.

d. 1. Titanite appears as fragments of unhexagonal crystals, honey-brown in colour. Analyses recalculated on the basis of 20 [O] are given in Table 7.

d. 2. Epidote appears in the form of allotropic grains replacing mainly plagioclase and biotite, in association with muscovite, titanite and spinel. It also forms microcrystalline covers around allanite grains. They are weakly pleochroic, with Y intense yellow-green, Z yellow-green and X greenish-yellow. Chemical analyses recalculated on the basis of 25 [O] are given in Table 8, along with the composition expressed in terms of the theoretical end member Ps.

d. 3. Allanite grains occur as porphyroclasts, or as inclusions. The porphyroclasts are strongly pleochroic, parallel to Y dark brown, almost opaque, parallel to Z brownish-red and parallel to X yellowish-grey. They are usually surfaced by an epidote cover.

Table 1. Representative chemical analyses of K-feldspars.

	FT10/104	FT10/108	FT10/111	FT6/5	FT6/6	FT6/8	FT6/11
SiO ₂	64.37	64.88	64.37	64.82	64.79	64.77	64.42
Al ₂ O ₃	18.16	18.26	18.06	18.17	18.06	18.08	18.07
FeO	0.03	0.01	0.04	0.04	0.01	0.01	0.03
CaO	0.01	0.01	0.01	0.01	0.01	0.01	0.01
Na ₂ O	0.38	0.37	0.36	0.33	0.26	0.33	0.3
K ₂ O	16.39	16.61	16.5	16.61	16.84	16.59	16.69
TOTAL	99.34	100.14	99.34	99.98	99.97	99.79	99.52
Z	15.99	15.98	15.97	15.98	15.97	15.98	15.97
X	4.04	4.06	4.06	4.05	4.08	4.05	4.08
Or	96.44	96.64	96.59	96.87	97.62	96.98	97.18
Ab	3.40	3.27	3.20	2.93	2.29	2.93	2.65
An	0.17	0.09	0.20	0.20	0.09	0.09	0.16
Number of ions on the basis of 32 [O]							
Si	12.00	12.00	12.00	12.01	12.02	12.02	12.00
Al	3.99	3.98	3.97	3.97	3.95	3.95	3.97
Fe	0.00	0.00	0.01	0.01	0.00	0.00	0.00
Ca	0.00	0.00	0.00	0.00	0.00	0.00	0.00
Na	0.14	0.13	0.13	0.12	0.09	0.12	0.11
K	3.90	3.92	3.93	3.93	3.98	3.93	3.97

Table 2. Representative chemical analyses of zoned K-feldspars.

	FT6/22c	FT6/22r	FT10/86c	FT10/86r	FT10/96c	FT10/96r
SiO ₂	64.92	64.86	65.07	63.52	62.63	64.11
Al ₂ O ₃	18.2	18.17	18.3	17.78	17.33	18.05
FeO	0.03	0.05	0.03	0.04	0.22	0.04
CaO	0.01	0.01	0.02	0.04	0.12	0.01
Na ₂ O	0.32	0.29	1.19	1.03	0.39	0.41
K ₂ O	16.44	16.61	14.99	15.25	15.16	16.16
TOTAL	99.92	99.99	99.6	97.66	95.85	98.78
Z	15.99	15.98	16.00	15.97	15.99	15.99
X	4.00	4.04	3.97	4.07	3.93	4.02
Or	96.97	97.18	89.04	90.37	94.76	96.09
Ab	2.87	2.58	10.74	9.28	3.71	3.71
An	0.17	0.24	0.22	0.35	1.53	0.21
Number of ions on the basis of 32 [O]						
Si	12.02	12.01	12.02	12.01	12.05	12.01
Al	3.97	3.97	3.98	3.96	3.93	3.98
Fe	0.00	0.01	0.00	0.01	0.04	0.01
Ca	0.00	0.00	0.00	0.01	0.02	0.00
Na	0.11	0.10	0.43	0.38	0.15	0.15
K	3.88	3.92	3.53	3.68	3.72	3.86
SiO ₂	64.61	64.82	64.44	68.76	67.65	64.80
Al ₂ O ₃	18.14	18.1	18.10	17.84	19.07	18.28
FeO	0.01	0.04	0.02	0.24	0.11	0.01
CaO	0.01	0.01	0.01	0.27	0.32	0.01
Na ₂ O	0.48	0.29	0.34	8.80	11.04	0.31
K ₂ O	16.24	16.4	16.53	3.82	1.15	16.62
TOTAL	99.49	99.66	99.44	99.73	99.34	100.03
Z	15.99	15.99	15.98	15.92	15.94	15.99
X	4.03	4.00	4.06	3.98	4.12	4.04
Or	95.62	97.18	96.85	21.73	6.29	97.16
Ab	4.30	2.61	3.03	76.08	91.84	2.75
An	0.09	0.21	0.13	2.19	1.87	0.09

Table 2, continue.

Number of ions on the basis of 32 [O]

Si	12.01	12.03	12.00	12.19	11.97	12.00
Al	3.97	3.96	3.97	3.73	3.98	3.99
Fe	0.00	0.01	0.00	0.04	0.02	0.00
Ca	0.00	0.00	0.00	0.05	0.06	0.00
Na	0.17	0.10	0.12	3.02	3.79	0.11
K	3.85	3.88	3.93	0.86	0.26	3.93

c : core r : rim

Table 3. Representative chemical analyses of plagioclases.

	FT10/103	FT10/107	FT6/40	FT8/9	FT8/10	FT8/13
SiO ₂	67.48	68.73	68.15	67.04	69.32	68.33
Al ₂ O ₃	19.64	19.15	19.32	19.84	19.64	19.46
FeO	0.02	0.11	0.05	0.41	0.04	0.02
CaO	0.5	0	0.24	0.45	0.21	0.18
Na ₂ O	10.05	11.99	11.79	11.36	12.1	11.44
K ₂ O	2.38	0.09	0.07	0.34	0.05	0.05
TOTAL	100.07	100.07	99.62	99.44	101.36	99.48

Z	15.98	15.96	15.97	15.97	15.96	16.01
X	4.07	4.10	4.08	4.11	4.11	3.94

Or	13.16	0.49	0.38	1.86	0.27	0.28
Ab	84.45	99.12	98.33	94.59	98.65	98.78
An	2.39	0.39	1.29	3.54	1.09	0.93

Number of ions on the basis of 32 [O]

Si	11.90	12.01	11.97	11.84	11.97	11.99
Al	4.08	3.94	4.00	4.13	4.00	4.02
Fe	0.00	0.02	0.01	0.06	0.01	0.00
Ca	0.09	0.00	0.05	0.09	0.04	0.03
Na	3.44	4.06	4.01	3.89	4.05	3.89
K	0.54	0.02	0.02	0.08	0.01	0.01

Table 4. Representative chemical analyses of zoned plagioclases.

	FT8/3r	FT8/3c	FT8/6r	FT8/6c
SiO ₂	68.76	68.42	68.87	67.64
Al ₂ O ₃	19.72	19.61	19.45	19.58
FeO	0.01	0.02	0.03	0.15
CaO	0.17	0.62	0.27	0.68
Na ₂ O	11.78	11.18	11.46	11.50
K ₂ O	0.06	0.05	0.08	0.05
TOTAL	100.50	99.90	100.16	99.60

Z	16.01	16.01	16.01	15.96
X	4.01	3.91	3.94	4.08

Or	0.33	0.28	0.45	0.27
Ab	98.84	96.68	98.16	96.05
An	0.82	3.04	1.39	3.68

Number of ions on the basis of 32 [O]

Si	11.94	11.94	11.99	11.88
Al	4.07	4.07	4.02	4.09
Fe	0.00	0.00	0.00	0.02
Ca	0.03	0.12	0.05	0.13
Na	3.97	3.78	3.87	3.92
K	0.01	0.01	0.02	0.01

c : core r : rim

Table 5. Representative chemical analyses of feldspars included in microcline or albite crystals.

	FT10/113	FT10/114	FT10/117	FT10/120	FT6/20	FT6/122
SiO ₂	64.80	64.74	64.63	64.93	63.21	63.51
Al ₂ O ₃	18.28	18.18	18.30	18.18	23.12	22.97
FeO	0.04	0.03	0.02	0.34	0.03	0.02
CaO	0.04	0.01	0.01	0.01	4.37	3.52
Na ₂ O ₃	1.12	1.35	2.05	1.63	9.10	9.85
K ₂ O	14.52	15.03	14.08	14.65	0.08	0.05
TOTAL	98.80	99.34	99.09	99.74	99.91	99.92

Z	16.04	15.99	15.99	15.96	16.01	16.02
X	3.85	4.04	4.07	4.08	3.97	4.05

Or	89.18	87.84	81.78	84.40	0.45	0.28
Ab	10.45	11.99	18.10	14.27	78.58	83.22
An	0.37	0.16	0.12	1.33	20.96	16.51

Number of ions on the basis of 32 [O]

Si	12.01	11.99	11.96	11.98	11.16	11.21
Al	4.03	4.00	4.02	3.98	4.85	4.82
Fe	0.01	0.00	0.00	0.05	0.00	0.00
Ca	0.01	0.00	0.00	0.00	0.83	0.67
Na	0.40	0.48	0.74	0.58	3.12	3.37
K	3.43	3.55	3.33	3.45	0.02	0.01

Table 7. Representative chemical analyses of titanites.

	FT-8/243	FT-8/238	FT-6/124
SiO ₂	33.12	32.86	32.56
TiO ₂	29.19	28.55	31.57
Al ₂ O ₃	7.35	7.12	6.82
FeO	1.36	2.91	1.54
CaO	28.76	28.13	27.43
Total	99.78	99.57	99.92

Number of ions on the basis of 20 [O]

Si	4.27	4.27	4.19
Ti	2.83	2.79	3.06
Al	1.12	1.09	1.03
Fe	0.15	0.32	0.17
Ca	3.97	3.92	3.78

Z	4.3	4.3	4.2
Y	4.1	4.2	4.3
X	4.0	3.9	3.8

Table 8. Representative chemical analyses of epidote crystals.

	FT10/105	FT10/105a	FT6/211
SiO ₂	38.81	38.04	38.12
TiO ₂	0.23	0.10	0.14
Al ₂ O ₃	20.48	20.77	21.81
Fe ₂ O ₃	14.82	15.07	13.5
Mn ₂ O ₃	0.76	0.48	0.64
CaO	22.10	22.83	23.37
Total	97.20	97.29	97.58

Number of ions on the basis of 25 [O]

Si	6.241	6.137	6.108
Ti	0.028	0.012	0.017
Al	3.882	3.949	4.119
Fe ³⁺	1.793	1.829	1.628
Mn ³⁺	0.093	0.059	0.078
Ca	3.808	3.946	4.012

Pistacite%	31.60	31.66	28.33
------------	-------	-------	-------

Z	6.24	6.14	6.11
Y	5.80	5.85	5.84
X	3.81	3.95	4.01

Table 6. Representative chemical analyses of micas.

	FT8/19	FT8/22	FT8/24	FT6/1	FT6/2	FT6/3	FT10/91	FT6/9	FT10/115	FT10/99	FT6/27	FT6/27a	FT6/14a	FT6/32a
SiO ₂	47.29	47.34	48.99	54.53	48.6	48	48.83	49.91	50.18	49.9	38.56	38.69	38.85	38.73
TiO ₂	0.13	0.69	0.21	0.24	0.43	0.4	0.29	0.27	0.04	0.07	0.08	0.08	0.13	0.12
Al ₂ O ₃	29.67	28.86	25.56	21.66	27.32	28.4	25.15	23.6	22.47	21.93	20.04	19.62	18.32	18.98
FeO	4.76	5.1	6.65	6.11	5.24	5.15	6.6	5.82	7.71	8.84	17.21	17.72	20.47	20.82
MnO	0.05	0.06	0.06	0.04	0.06	0.06	0.07	0.07	0.08	0.09	0.25	0.26	0.26	0.22
MgO	1.4	1.53	1.53	2.45	2.11	1.85	2.41	2.88	2.68	2.39	8.59	8.84	8.32	8.27
Na ₂ O	0.28	0.34	0.13	0.08	0.21	0.21	0.14	0.08	0.09	0.1	0.06	0.06	0.08	0.11
K ₂ O	10.92	10.95	10.67	9.3	10.62	10.87	10.87	11.17	11.05	10.83	9.35	9.52	9.68	9.63
Total	94.5	94.87	93.8	94.41	94.59	94.94	94.36	93.8	94.3	94.15	94.14	94.79	96.11	96.88

Number of ions on the basis of 22 [O]

Si	6.479	6.483	6.808	7.382	6.653	6.556	6.765	6.933	6.996	7.005	5.806	5.809	5.84	5.78
Ti	0.013	0.071	0.022	0.024	0.044	0.041	0.03	0.028	0.004	0.007	0.009	0.009	0.01	0.01
Al	4.791	4.658	4.187	3.456	4.408	4.572	4.107	3.864	3.692	3.629	3.557	3.472	3.25	3.34
Fe	0.545	0.584	0.773	0.692	0.6	0.588	0.765	0.676	0.899	1.038	2.167	2.225	2.57	2.60
Mn	0.006	0.007	0.007	0.005	0.007	0.007	0.008	0.008	0.009	0.011	0.032	0.033	0.03	0.03
Mg	0.286	0.312	0.317	0.494	0.431	0.377	0.498	0.596	0.557	0.5	1.928	1.978	1.87	1.84
Na	0.074	0.09	0.035	0.021	0.056	0.056	0.038	0.022	0.024	0.027	0.018	0.017	0.02	0.03
K	1.909	1.913	1.892	1.606	1.855	1.894	1.921	1.979	1.965	1.94	1.796	1.823	1.86	1.83

Z	8	8	8	8	8	8	8	8	8	8	8	8	8	8.00
Y	4.12	4.12	4.11	4.05	4.14	4.14	4.17	4.11	4.16	4.19	5.5	5.53	5.58	5.60
X	1.98	2	1.93	1.63	1.91	1.95	1.96	2	1.99	1.97	1.81	1.84	1.88	1.87

d. 4. Zircon appears in hypidiomorphic crystals, with an elongation ratio averaging 2. Some crystals present zoning and darker core.

d. 5 Garnet occurs as small isodiametric isotropic crystals. It was usually found in secondary mineral aggregates, as a product of biotite and feldspar alteration. Representative analyses recalculated on the basis of 12 [O] are given in Table 9 along with the composition expressed in terms of the theoretical end members.

d. 6. Only a few apatite crystals were observed.

d. 7. Magnetite was found in hypidiomorphic grains, usually in contact with muscovite, epidote and other biotite alteration products. Small goethite grains were ob-

Table 9. Representative chemical analyses of garnets.

	FT-8/233	FT-8/235	FT-6/122
SiO ₂	36.42	36.81	37.8
TiO ₂	1.37	1.47	1.52
Al ₂ O ₃	21.44	20.39	21.36
FeO	25.16	26.62	24.11
MnO	0.21	0.2	0.36
MgO	0.14	0.02	0.04
CaO	15.38	14.65	15.22
Na ₂ O	0.06	0.02	0.02
K ₂ O	0.05	0.01	0.03
Total	100.23	100.19	100.46

Number of ions on the basis of 12 [O]

Si	2.892	2.938	2.968
Ti	0.082	0.088	0.090
Al ^{IV}	0.000	0.000	0.000
Al ^{VI}	2.023	1.933	1.992
Fe	1.671	1.777	1.583
Mn	0.014	0.014	0.024
Mg	0.017	0.002	0.005
Ca	1.309	1.253	1.280
Na	0.009	0.003	0.003
K	0.005	0.001	0.003

Z	2.89	2.94	2.97
Y	2.10	2.02	2.08
X	3.01	3.05	2.89

Pyr	0.6	0.1	0.2
Alm	55.5	58.3	54.7
Spess	0.5	0.4	0.8
Andr	0.0	0.0	0.0
Gross	43.5	41.1	44.3

served as an alteration product of magnetite. Representative analyses of magnetite crystals are given in Table 10.

Table 10. Representative chemical analyses of magnetite crystals.

	FT10/100	FT6/15	FT6/16
TiO ₂	0.04	0.17	0.17
Al ₂ O ₃	0.11	0.04	0.02
Cr ₂ O ₃	0.01	0.02	0.02
Fe ₂ O ₃	67.74	68.14	67.96
FeO	31.72	31.91	31.83
MnO	0.07	0.04	0.10
MgO	0.01	0.02	0.01
Total	99.70	100.35	100.11

Number of ions on the basis of 4 [O]

Ti	0.001	0.005	0.005
Al	0.005	0.002	0.001
Cr	0.000	0.001	0.001
Fe ³⁺	1.973	1.972	1.972
Fe ²⁺	1.027	1.026	1.026
Mn	0.002	0.001	0.003
Mg	0.001	0.001	0.001

Z	1.98	1.98	1.98
X	1.03	1.03	1.03

	FT6/19	FT8/8	FT8/11
TiO ₂	0.14	0.10	0.12
Al ₂ O ₃	0.03	0.03	0.00
Cr ₂ O ₃	0.03	0.04	0.01
Fe ₂ O ₃	68.15	67.76	68.38
FeO	31.91	31.73	32.02
MnO	0.03	0.12	0.03
MgO	0.01	0.01	0.04
Total	100.31	99.79	100.61

Number of ions on the basis of 4 [O]

Ti	0.004	0.003	0.003
Al	0.001	0.001	0.000
Cr	0.001	0.001	0.000
Fe ³⁺	1.973	1.973	1.974
Fe ²⁺	1.027	1.027	1.028
Mn	0.001	0.004	0.001
Mg	0.001	0.001	0.002

Z	1.98	1.98	1.98
X	1.03	1.03	1.03

Petrography

Granite is the only rock type of the intrusion. It is light grey, dark grey to greenish-grey in colour, with a partly porphyritic structure and strong foliation. Late magmatic, or hydrothermal activity has affected the plutonic rocks causing decomposition of primary feldspar and biotite. Modal analyses of the studied rocks are given in Table 11.

In thin section the rock, though strongly tectonised, it still preserves its original granitic texture. It is composed of K-feldspar quartz, plagioclase biotite and allanite porphyroclasts, surrounded by fine fragments of the same minerals and other primary phases such as zircon, apatite and titanite, along with recrystallised and secondary formed minerals such as quartz, muscovite and epidote.

Table 11. Modal analyses of representative samples

	FT-3	FT-9	FT-8	FT-10	FT-11	FT-12
	n=2582	n=1953	n=2841	n=2255	n=2161	n=1646
Quartz	32.7	37.8	37.4	37.3	34.4	30.4
Plagioclase	18.5	17.3	7.7	14.1	14.2	14.5
Microcline	40.5	38.2	40.2	41.1	35.2	41.3
Muscovite	7.0	4.5	12.3	5.7	8.5	3.3
Biotite	0.2	tr	0.8	0.4	5.3	8.2
Epidote	tr	0.7	0.1	0.5	0.5	0.5
Titanite	0.1	0.5	0.4	0.4	0.8	1.2
Opaque	1.0	0.7	1.1	0.1	0.5	0.4
Garnet	-	tr	-	tr	-	-
Allanite	tr	0.3	tr	0.4	0.6	0.1
Zircon	tr	tr	tr	tr	tr	tr
Apatite	-	tr	tr	-	tr	-

n = counts tr = traces

Vein-like aggregates composed of fine grained recrystallised quartz, small fragments of K-feldspar, muscovite flakes and secondary mineral grains, cross the rock parallel to foliation surfaces, arching around the porphyroclasts. All the intermediate grain sizes between the large porphyroclasts and the cryptocrystalline fragments are present, with no dominant size, so that the structure of the rock relative to the grain size can be characterised as successive porphyroclastic.

Chemical results

The major element analytical results along with the CIPW norms of representative analyses are given in Table 12 and the trace along with the rare earth element results are given in Tables 13 and 14.

In Figs. 3 and 4 the geochemical trend is shown in the plots of various major and trace elements v. SiO₂. Mantle and ORG normalised plots, as well as trace element diagrams for the discrimination of the geotectonic environment are shown in Figs. 5 - 7. Finally, chondrite normalised REE patterns are drawn in Fig 8.

Age determination

Rb-Sr whole rock and mica analyses were carried out on 2 samples. The Rb-Sr analytical results as well as age determinations of the studied rocks are listed in Table 15. The long-time reproducibility for the ⁸⁷Sr/⁸⁶Sr ratio

gave a mean value of 0.71033·5 (1σ, n=29). Rb and Sr contents have been measured by isotopic dilution method, using 98 % ⁸⁷Rb and 99.9 % ⁸⁴Sr spikes, respectively.

Age determinations from muscovite concentrates and the corresponding whole rocks gave values ranging from 273 to 225 Ma (Table 15).

Some ages obtained by mica concentrates represent rejuvenated Rb-Sr systems of muscovites, affected by various tectonic events. Considering the high whole rock Rb/Sr ratio we can assume that these strongly differentiated granites reacted probably as an open system to these events regarding their Rb and Sr contents. For this reason, in addition to the high Rb/Sr values, the (⁸⁷Sr/⁸⁶Sr)_i values diverge significantly from the relative values of other neighbouring plutonic rocks (Verdikoussa, Diava and Deskati plutonic complexes) and they are not reported. In any case it seems reliable that its emplacement took place during Variscan orogenesis.

Discussion - Conclusions

From the mineral chemistry we can reveal some essential features of the plutonic rocks.

The K-feldspar is essentially microcline (Or = 97.62 - 96.44 %) and plagioclase is represented by albite and acid oligoclase (Ab = 99.12 to 84.45 %). There is a lack of calcium rich plagioclase in the studied granitic rocks, due to the decomposition of the primary plagioclase.

Table 12 Representative major element analyses of the studied rocks.

	FT8	FT5	FT3	FT7	FT1	FT2	FT16
SiO ₂	78.48	78.45	78.39	78.26	78.22	78.08	77.62
TiO ₂	0.20	0.18	0.17	0.20	0.20	0.22	0.24
Al ₂ O ₃	11.20	11.46	11.47	11.95	11.70	11.82	11.72
FeO	1.19	1.16	1.14	1.29	1.43	1.62	1.31
MnO	0.01	0.00	0.00	0.01	0.01	0.01	0.00
MgO	0.22	0.21	0.20	0.25	0.27	0.22	0.18
CaO	0.41	0.12	0.20	0.37	0.17	0.17	0.12
Na ₂ O	3.62	2.62	2.38	2.69	2.87	2.49	2.46
K ₂ O	4.94	5.64	5.46	5.58	5.23	5.17	5.57
P ₂ O ₅	0.04	0.03	0.02	0.04	0.04	0.03	0.02
L.O.I.	0.53	0.31	0.65	0.44	0.52	0.27	0.45
Total	100.84	100.18	100.10	101.07	100.65	100.09	99.69

Norm wt %

Ap	0.07	0.05	0.04	0.07	0.07	0.05	0.04
Il	0.32	0.29	0.27	0.32	0.32	0.36	0.39
Or	26.89	30.99	30.13	30.43	28.66	28.41	30.87
Ab	29.95	21.89	19.98	22.30	23.85	20.84	20.70
An	0.05	0.39	0.81	1.47	0.56	0.62	0.45
C	0.00	0.57	0.84	0.57	0.70	1.19	0.94
WoDi	0.81	0.00	0.00	0.00	0.00	0.00	0.00
EnDi	0.22	0.00	0.00	0.00	0.00	0.00	0.00
FsDi	0.58	0.00	0.00	0.00	0.00	0.00	0.00
EnHy	0.48	0.67	0.64	0.79	0.86	0.70	0.58
FsHy	1.24	1.79	1.79	2.01	2.27	2.57	1.99
Q	39.40	43.36	45.50	42.02	42.72	45.25	44.05

	FT4	FT6	FT9	FT10	FT12	FT11	FT13
SiO ₂	77.44	77.02	76.82	76.73	75.26	74.92	74.08
TiO ₂	0.26	0.20	0.19	0.28	0.32	0.30	0.32
Al ₂ O ₃	11.72	12.23	11.89	12.35	12.33	12.48	12.40
FeO	1.13	1.28	1.58	1.40	1.89	1.67	2.25
MnO	0.00	0.00	0.01	0.01	0.02	0.01	0.22
MgO	0.19	0.25	0.24	0.26	0.44	0.38	0.55
CaO	0.15	0.12	0.46	0.53	0.52	0.50	0.63
Na ₂ O	2.89	2.97	2.93	2.73	2.93	3.61	2.85
K ₂ O	5.40	5.55	5.42	5.18	5.81	5.32	5.19
P ₂ O ₅	0.03	0.03	0.04	0.04	0.07	0.05	0.08
L.O.I.	0.47	0.86	0.43	0.45	0.54	0.65	0.65
Total	99.69	100.51	100.00	99.95	100.12	99.89	99.20

Norm wt %

Ap	0.05	0.05	0.07	0.07	0.13	0.09	0.15
Il	0.42	0.32	0.31	0.45	0.52	0.49	0.52
Or	29.91	30.67	29.89	28.61	32.18	29.55	29.03
Ab	24.28	24.97	24.56	22.91	24.70	30.48	24.20
An	0.53	0.39	1.90	2.23	2.02	1.99	2.50
C	0.59	0.75	0.30	0.88	0.27	0.00	0.73
WoDi	0.00	0.00	0.00	0.00	0.00	0.04	0.00
EnDi	0.00	0.00	0.00	0.00	0.00	0.01	0.00
FsDi	0.00	0.00	0.00	0.00	0.00	0.02	0.00
EnHy	0.61	0.80	0.77	0.84	1.41	1.21	1.78
FsHy	1.64	1.99	2.58	2.11	2.95	2.54	4.00
Q	41.97	40.05	39.62	41.89	35.82	33.58	37.09

Table 13. Representative trace element analyses in ppm.

	FT1	FT2	FT3	FT4	FT5	FT6	FT16
Sc	10	8	6	3	11	9	7
V	13	17	12	11	16	13	15
Cr	7	21	7	1	7		--
Co	53	62	72	49	46	47	47
Cu	2.5	2.8	0.6	0.1	1.6	3	--
Ba	294	288	252	264	269	270	251
La	31	32	14	37	26	28	24
Ce	38	45	23	79	41	54	57
Nd	23	28	11	30	18	23	26
Nb	18	20	13	14	13	14	13
Zr	166	194	123	132	122	135	138
Y	46	21	23	41	29	33	36
Sr	34	37	31	20	29	29	27
Rb	263	278	273	267	246	245	240
Th	22	25	21	28	22	26	25
Ga	16	17	15	15	16	17	17
Zn	35	41	12	15	15	20	16

	FT7	FT8	FT9	FT10	FT11	FT12	FT13
Sc	6	6	6	7	5	4	3
V	17	15	14	13	21	19	29
Cr	--	3	0.3	1	14	20	7
Co	46	48	31	32	21	30	26
Cu	--	1.6	3.1	1.4	0	0	0
Ba	320	258	305	289	238	227	260
La	32	31	32	31	33	37	40
Ce	57	66	63	62	68	78	79
Nd	23	25	23	25	27	30	33
Nb	13	15	13	13	15	14	13
Zr	153	155	143	151	210	229	221
Y	38	42	43	42	46	56	54
Sr	43	30	39	42	61	43	63
Rb	282	288	274	269	312	275	292
Th	23	23	21	23	36	33	33
Ga	16	16	16	16	19	18	18
Zn	21	18	44	63	16	26	25

Table 14. Representative REE analyses in ppm.

	La	Ce	Pr	Nd	Sm	Eu	Gd	Dy	Er	Yb	Lu
FT8	10.9	21.1	3.42	13	2.6	0.23	2.5	3.05	1.97	1.96	0.28
FT10	33.2	68.4	8.5	33.6	5.3	0.68	5.32	5.34	3.23	3.13	0.41
FT13	26.4	55.5	7.3	27	4.8	0.56	4.93	5.56	3.59	3.59	0.47

Table 15. Rb-Sr geochronological data of the studied plutonic rocks.

Sample	Material	Rb ppm	Sr ppm	$^{87}\text{Rb}/^{86}\text{Sr}$	$^{87}\text{Sr}/^{86}\text{Sr}$ ($\pm 2\sigma$)	Age Ma ($\pm 2\sigma$)
FT-5	W.ROCK	231	29.8	22.638	0.84951 \pm 3	
	MUSCOVITE	946	9.1	335.652	1.85192 \pm 6	225 \pm 2
FT-8	W.ROCK	87	62	4.106	0.76916 \pm 2	
	MUSCOVITE	682	15.1	138.342	1.2913 \pm 2	273 \pm 3

Normal zoning of the sodium feldspar is common. As an example, sample FT8/6 (Table 4) presents an Ab content of 96.05 % in the core (analysis FT8/6c), while the rim composition is sodium enriched with an Ab content 98.16 % (analysis FT8/6r).

This plagioclase zoning cannot be considered indicative of its origin, as it is not exclusively a primary characteristic of the mineral. It is also the result of the extended decomposition that it is not uniform, but advances progressively from the edges of the crystal towards the core, along cracks, or cleavage and twinning surfaces.

Normal zoning is also common in K-feldspar. As an example, sample FT10/96 (Table 2) presents in the core an Or % content of 94.76 (analysis FT10/96c), while the rim is potassium enriched (Or % 96.09 analysis FT10/96r). A common feature is the development of a thin albite rim around microcline crystals (analyses FT10/118c, FT10/118r, Table 2), while the development of a thin K-feldspar rim around plagioclase crystals is less common (analyses FT10/109c, FT10/109r Table 2). The smaller K-feldspar crystals are usually twinning free, indicating a selective recrystallisation of the neighbouring grains.

Both, sodium (Ab % = 78.58 - 83.22) and potassium (Or % = 81.78 - 89.18) feldspars grains up to 0.5 mm in length are included in larger albite and microcline crystals. Plagioclase inclusions have more calcic composition than the host albite crystals, while K-feldspar inclusions are potassium depleted and sodium richer, compared to the large microcline crystals.

The analysed biotites can be considered Ti depleted, as TiO₂ percentage is always lower than 0.1. But the small anatase and hematite grains, that can be observed along the biotite cleavage, are exsolution products indicative of an originally Fe, Ti rich biotite. The high elongation ratios measured indicate a crystallisation at low temperatures.

Muscovite must have been crystallised meta-tectonically as there are small muscovite flakes that are enclosed in recrystallised quartz grains, while there are not any muscovite inclusions in primary phases such as K-feldspar.

There are a few large muscovite crystals protected among the porphyroclasts so that they are not tectonically affected. The development of these large muscovite crystals is probably due to a selective crystallisation of fine sericite grains. The majority of muscovite flakes have an orientation and they are strongly affected by a late tectonism.

Epidote composition is usually expressed in terms of the theoretical pistacite end member: $P_s = 100 \cdot Fe^{3+} / (Fe^{3+} + Al)$. Natural epidote composition rarely exceeds P_{s33} (DEER et al. 1986). Epidotes of the studied samples present P_s % value 31.6.

Garnet is almandine (Alm = 54.7 - 58.3 %) containing appreciable amounts of the grossularite molecule (Gross. = 41.1-44.3 %). Both, garnet and titanite are partly primary and partly the result of biotite and plagioclase decomposition.

Magnetite is the only spinel present in the rocks studied. In some cases it is oxidised to hematite.

From the mineralogical characteristics described above, the successive crystallisation can be depicted. The oldest authigenic mineral phases of the studied rocks are zircon, apatite, allanite and partly titanite, which were formed during a primary stage of the magma crystallisation. Plagioclase and K-feldspar crystallised consequently. The formation of the latter is partly over-

lapped and followed by the primary quartz and biotite crystallisation. At the same time the Na-component of the alkali feldspar was separated causing the perthite formation. During tectonism a recrystallisation of quartz took place, while from the existing liquid phase crystallised fine quartz, K-feldspar and muscovite, filling the cracks and the fissures among the porphyroclasts.

Hydrothermal alteration caused the biotite and plagioclase decomposition, giving rise to secondary quartz, muscovite, titanite, garnet and magnetite.

In Fig. 2 the possible crystallisation sequence for the Fotino granitic rocks is presented.

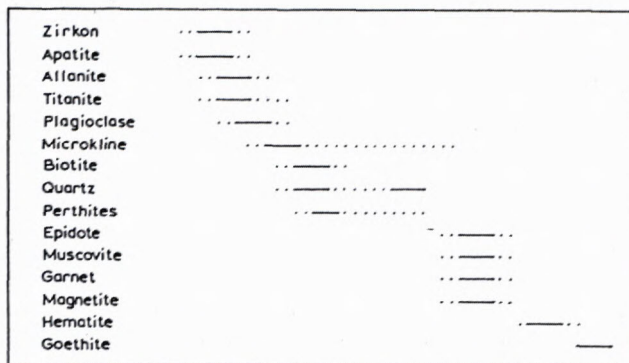


Fig. 2 Possible crystallisation sequence for the Fotino granitic rocks

From the rock chemistry some important petrogenetic features of the studied rocks can also be depicted.

All the studied samples of the Fotino granite show S type characteristics, as muscovite is the main mica present, plagioclase is albite and acid oligoclase (Ab = 99.12 to 84.45 %), CaO content is low, the Rb/Sr ratio is high (4.6 - 13.4), normative anorthite content is low, ranging from 0.05 - 2.50, Na₂O content ranges from 2.4 to 3.6 and for K₂O averaging 5.4.

The molar ratio $Al_2O_3 / (CaO + Na_2O + K_2O)$ ranges from 0.93 to 1.19, so as normative C values range from 0.0 to 1.2.

S-type granitoids in Greece have been reported in Macedonia (N. Greece) and in Paros island, (Aegean Sea). In N Greece the Sochos plagiogranite and the Arnea leucogranite, both belonging to the Circum Rhodope belt of the Hellenides, show typical S-type characteristics (BALTATYIS & al. 1992). In Paros island, which belongs to the Attico-Cycladic unit, ALTHER (1981) and ALTHER et al. (1982) reported a granitic body also presenting S-type properties. Typical S-type characteristics are also described for the Deskati plutonic rocks (KATERINOPOULOS et al. 1994)

The major element analytical results of the Fotino granites, plotted in Harker variation diagrams (Fig. 3), depict a negative correlation for FeO, MgO, TiO₂ and CaO in relation to SiO₂, while Al₂O₃ and total alkalis do not show any significant variation.

Concerning the trace elements, a positive correlation for Ba and a negative one for Nd, Y, Rb, Sr, V and Zr are shown in the plots of the trace elements v. SiO₂ (Fig. 4). Probably, part of the mobile elements was washed away during the tectonism and the hydrothermal alteration, bringing about the S type characteristics mentioned.

In terms of the criteria proposed by PEARCE et al. (1984) the studied samples exhibit the geochemical

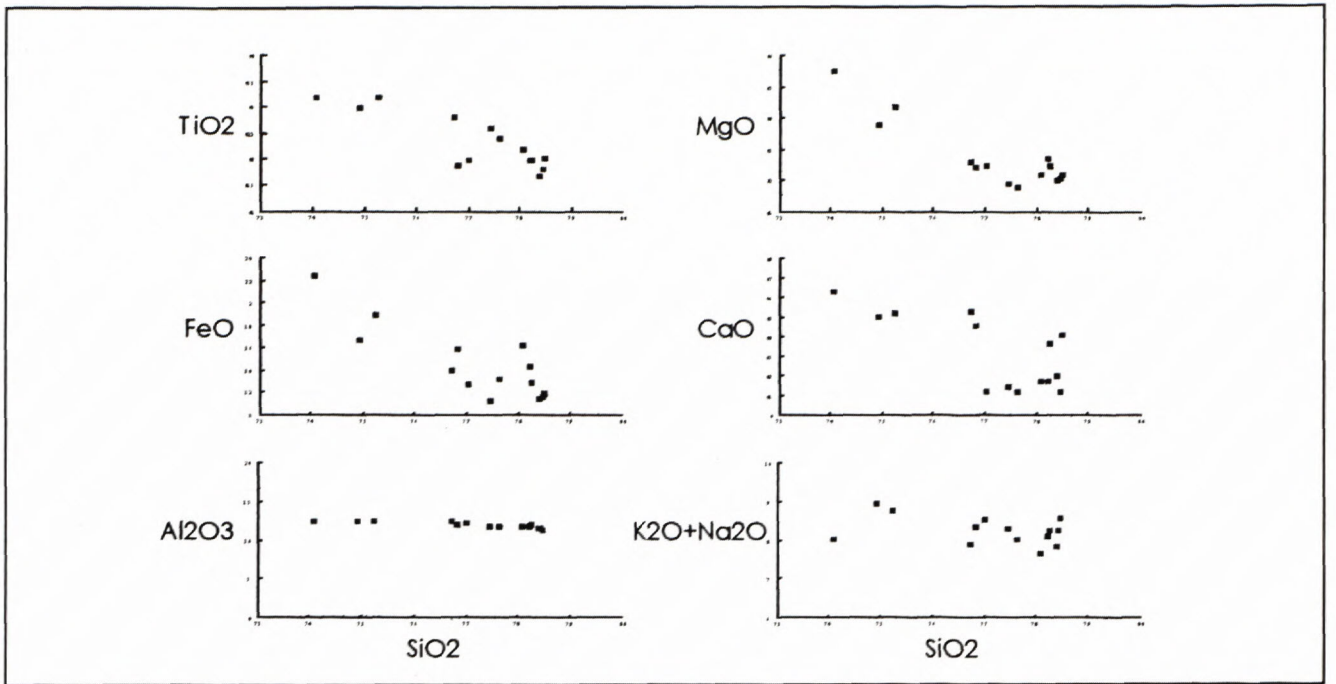


Fig. 3 Major element variation diagrams.

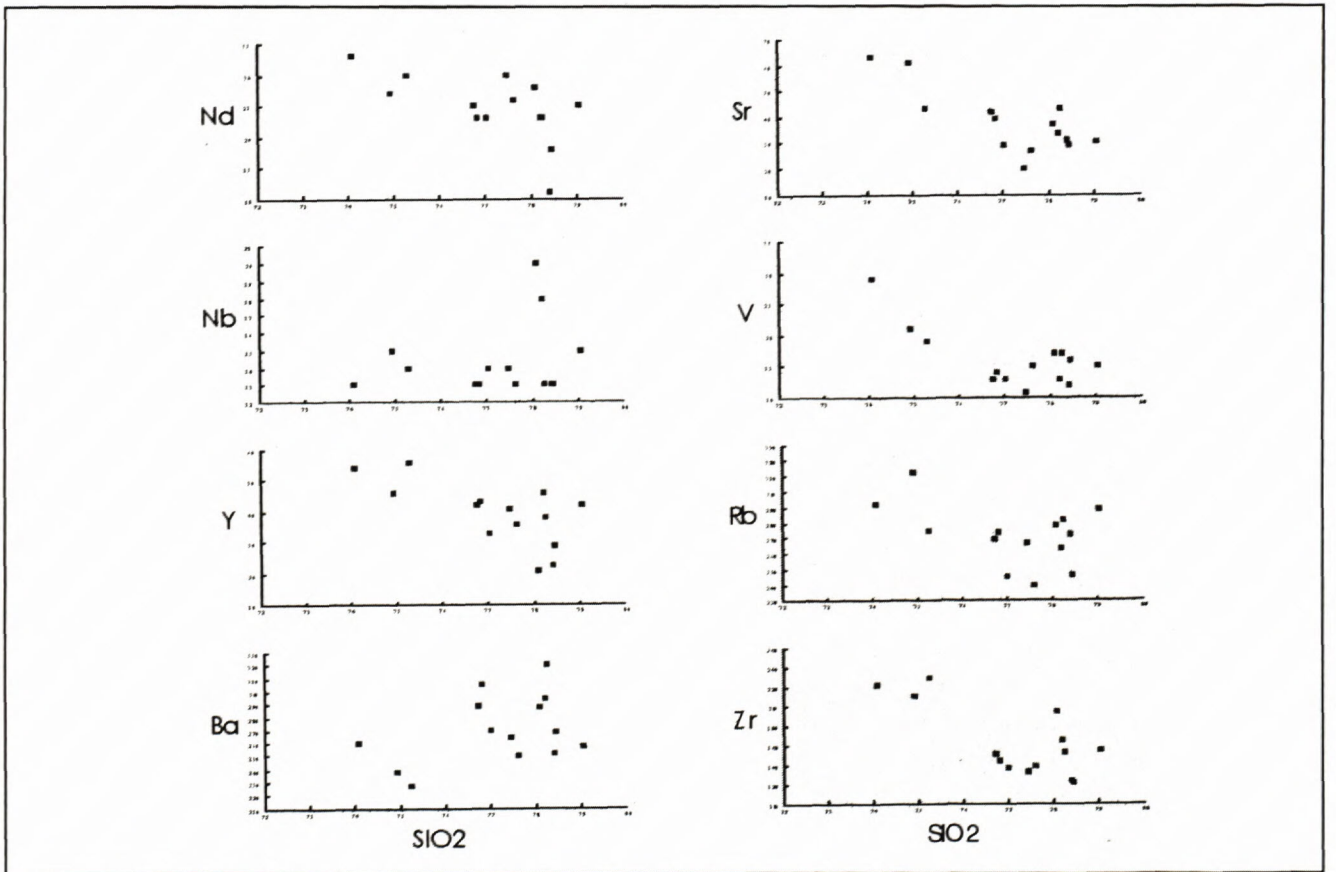


Fig. 4 Trace element variation diagrams.

characteristics that can be attributed to both granites formed in a Volcanic Arc environment, or Within Plate granites. The ORG normalised geochemical diagrams for representative samples (Fig. 5) have shapes similar to the plots of typical Volcanic Arc granites and especially

the granite from Chile (PEARCE & al. 1984). They are characterised by strong enrichment in K, Rb, Ba, and Th, relative to Nb, Ce, Zr, Sm, Y, and Yb, negative anomalies for Nb, Ba and Zr and low Y and Yb values relative to the normalising compositions.

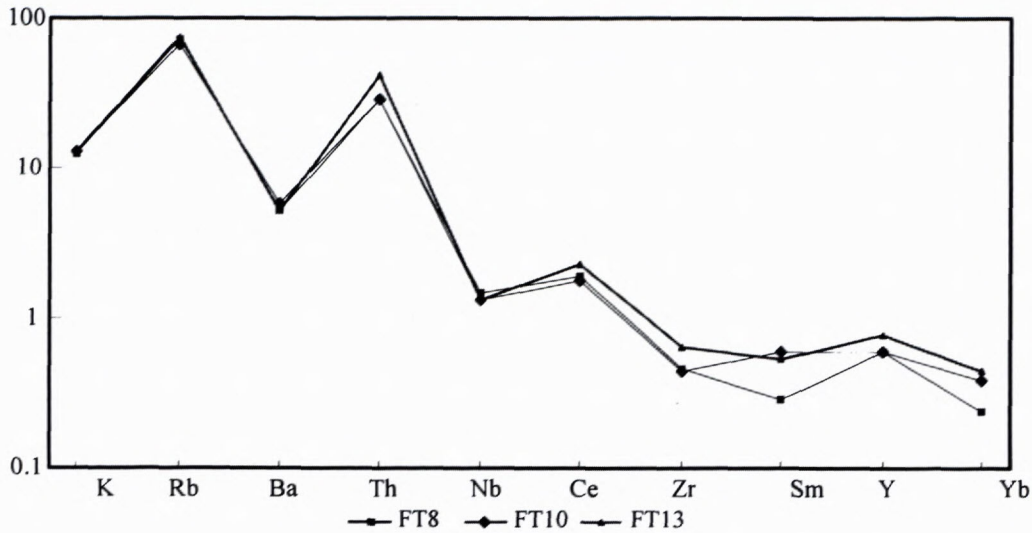


Fig. 5 Ocean Ridge Granites normalised plots of representative samples (after PEARCE et al. 1984).

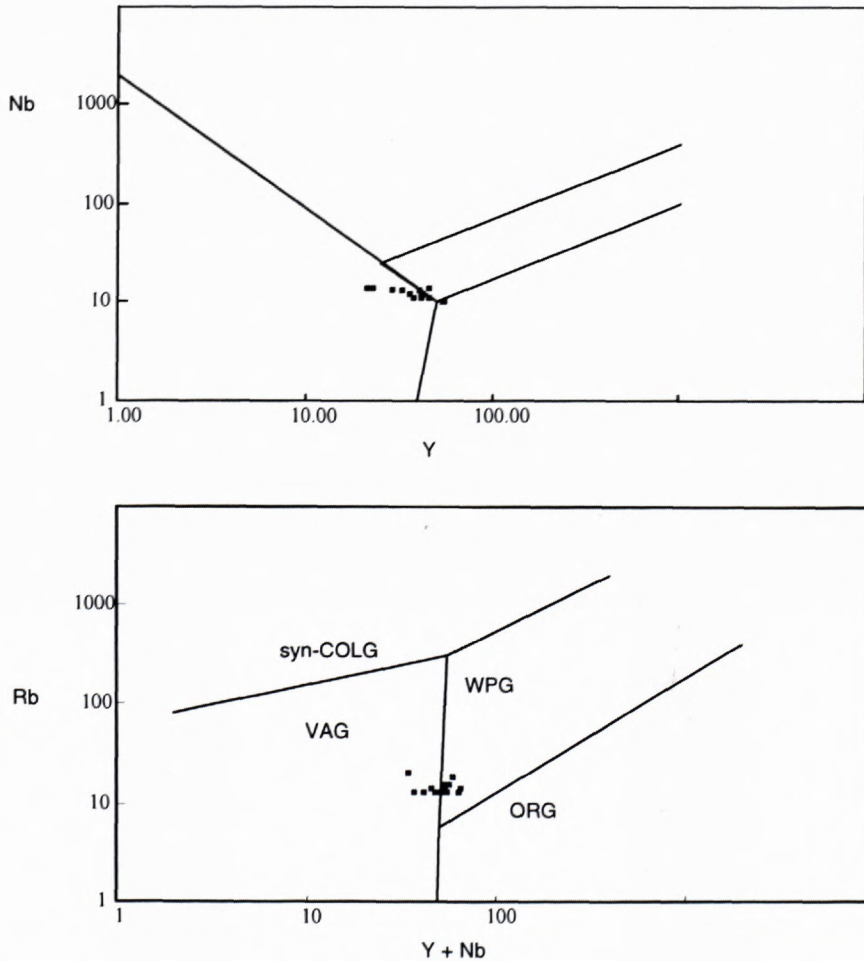


Fig. 6 Nb v. Y and Rb v. (Y + Nb) plots (after PEARCE et al. 1984).

At the same time the studied rocks could be considered Within Plate granites, according to the criteria proposed by PEARCE et al. (1984), as their ORG normalised geochemical patterns are similar to that of Skaergaard granite, which is considered a typical Within Plate intrusion. They have high ratios of Rb and Th relative to Nb, a characteristic of "crust dominated" pattern and flat trends from Zr to Yb with values close to the normalising ones. Figure 6 shows the Nb v. Y and the Rb v. (Y+Nb) plots (proposed by PEARCE et al. 1984) for the discrimination of the geotectonic environment of granitic rocks. The studied samples plot in both the VAG and the WPG fields.

The same geochemical characteristics are depicted from the relative diagrams of the Deskati granitic rocks (KATERINOPOULOS et al. 1994)

In Fig. 7 the mantle normalised large ion lithophile and high strength element spider-diagrams (WOOD & al. 1979) for representative samples are shown. All of them present geochemical characteristics such as high

LIL/HFS element ratios and marked negative Nb, P and Ti anomalies, typical of all subduction zone magmas, precluding the within-plate genesis partly indicated by the diagrams in Figs. 5 and 6.

Those characteristics indicate a relation of the studied plutonic rocks to a subduction geotectonic environment, in accordance with the petrographic observations mentioned, which indicate a syn-tectonic intrusion.

The same characteristics are depicted from the relative diagrams of the Verdikoussa and Deskati granites (KATERINOPOULOS 1994, KATERINOPOULOS et al. 1994)

The plot of some samples in the WPG field of the Nb v. Y and Rb v. (Y+Nb) plots may be attributed to various types of alteration (PEARCE et al., 1984), which are common in the studied rocks.

In relation to other granitic rocks in Greece (BALTAZIS et al 1992, KATERINOPOULOS et al 1992) the studied samples have larger Ba, Sr, Nb, P and Ti negative anomalies. Average continental crust has quite significant nega-

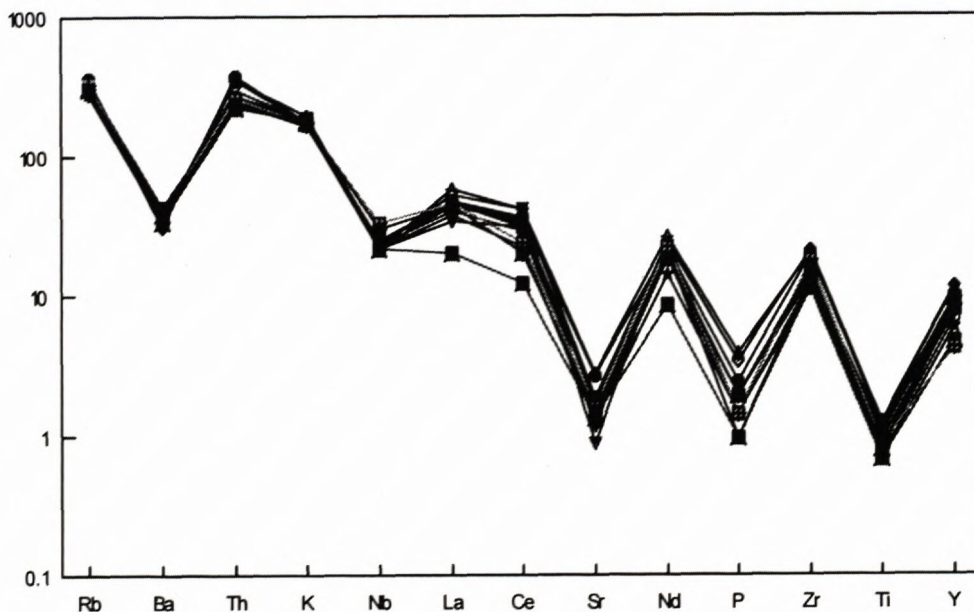


Fig. 7 Mantle normalised LIL and HFS element plots of representative samples (after WOOD et al. 1979).

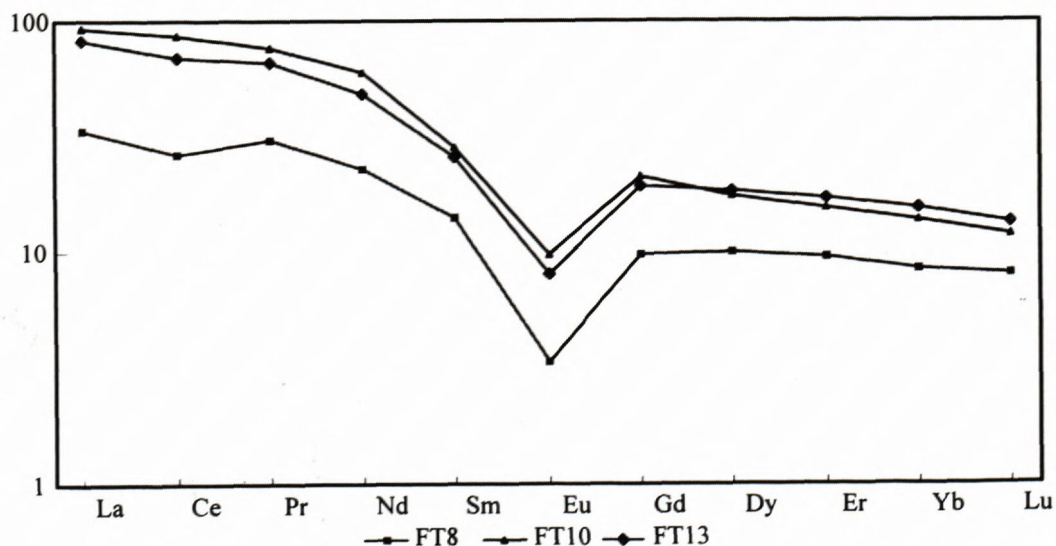


Fig. 8 Rare Earth Element patterns of selected samples (normalisation after HASKIN & al. 1968).

tive anomalies for these elements (JONES et al. 1992), so we can assume an increased crustal involvement to the composition of the parental magma.

The chondrite normalised (HASKIN et al 1968) REE patterns of selected samples (Fig. 8) show relatively high LREE/HRRE ratios and strong Eu negative anomalies, indicating that the distribution of the REE was strongly controlled by the fractionation of feldspars.

In the case of the Deskati and Fotino plutons their formation can be due to a number of diverse mechanisms including crustal anatexis and fractional crystallisation, either, or not combined with assimilation. However, there are several indications that they derived from different parental magma(s) originating the Diava and Verdikoussa magmatic suite, while they probably have a common origin with the Deskati plutonic rocks.

Concerning the age of the emplacement, we can conclude it took place during the Variscan time, according to the analytical data. The same age has been determined for the Deskati plutonic rocks occurring north of the studied area, the Verdikoussa and Diava plutons situated E of the studied pluton, the Varnoundas and Baba mountain plutonic rocks lying NW of the studied area (KATERINOPOULOS et al. 1992) as well as for Pieria granites, situated NE of the studied plutons (SCHERMER et al. 1989).

Since the Permian period the Palaeo-Tethys ocean started to develop between Eurasia and Gondwana. During Permo-Triassic, the Cimmerian continent had been separated and broke into smaller pieces (MOUNTRAKIS 1983), so that the Palaeo-Tethys and Neo-Tethys oceans were created at both sides of the North Pelagonian zone, possibly representing the north-western part of the Cimmerian continent (KORONEOS 1991). During that period a subduction zone should have been developed in the area, giving rise to an extended calc-alkaline plutonism.

Acknowledgements

The authors are grateful to Prof. J. TARNEY, University of Leicester, for making available the analytical facilities in the Department of Geology.

References

- ALThER, R. (1981). Zur petrologie der miozanen granitoiden der zentralagais (Griechenland). *Habil-Schrift Techn.Univ. Braunschweig*, 218 p.
- ALThER, R., KREUZER, H., WENDT, I., LENZ, H., WAGNER, G.A., KEKKER, J., HARRE, W. & HOHNDORF, A. (1982) A Late Oligocene/Early Miocene high temperature belt in the Attic-Cycladic crystalline complex (SE Pelagonian, Greece). *Geol. Jb.*, E23, 97-164.
- ANDERSON, L. J. (1980). Mineral equilibria and crystallisation conditions in the Late Precambrian Wolf River Rapakivi massif, Wisconsin., *Am. J. Sci.*, 280, p. 289-332
- BALTATZIS, E., ESSON, J. & MITROPOULOS, P. (1992) Geochemical characteristics and petrogenesis of the main granitic intrusions of Greece: an application of trace element discrimination diagrams. *Min. Mag.*, 56, p. 487 - 501.
- DEER, W. A., HOWIE, R. A. & ZUSSMAN, J. (1986). *Rock forming minerals*, 1B. Longman S & T, New York, 629 p.
- HASKIN, L.A., HASKIN, M.A., FRAY, F.A. & WILDEMAN, D. R. (1968). Relative and absolute terrestrial abundances of the rare earths. In L.A. Ahrens ed. *Origin and distribution of the elements*. Pergamon, Oxford, p. 889 - 912.
- JONES, C.A., TARNEY, J., BAKER, J. & GEROUKI, F. (1992). Tertiary granitoids of Rhodope, N. Greece: magmatism related to extensional collapse of the Hellenic orogen?. *Tectonoph.*, 210, p. 1 - 21.
- KATERINOPOULOS, A. (1994) *Petrology and Chemical Characteristics of the Verdikoussa Granitic Rocks, Thessaly, Greece*. *Ann. Geol. Pays Hell.* (In print)
- KATERINOPOULOS, A., KYRIAKOPOULOS, K. & MARKOPOULOS, T. (1992) Distribution in time and space of the acid plutonic complexes in Greece. *International IGCP Congress No 276. Paleozoic Geodynamic Domains and their Alpidic Evolution in Tethys*. Granada.
- KATERINOPOULOS, A., KOKKINAKIS, A. & KYRIAKOPOULOS, K. (1994) *Petrology and Chemical Characteristics of the Deskati Granitic Rocks, Thessaly, Greece*. 7th Congress. *Geol. Soc. Greece, Thessaloniki*.
- KATSIKATSOS, G. & MIGOIS, G., Triantaphyllis, M., Mettos, A., (1986). Geological structure of internal Hellenides. *Geol. Geoph. Res.*, Sp. issue, p. 191-212.
- KILIAS, A. & MOUNTRAKIS, D. (1989). The Pelagonian Nappe. Tectonics, metamorphism and magmatism. *Bull. Geol. Soc. Greece*, 23/1 p. 29-46.
- KORONEOS, A. (1991). *Mineralogy, Petrology and Geochemistry of the East Varnoundas plutonite (N. W. Macedonia)* Ph.D. Thesis, University of Thessaloniki, 414pp.
- MARSH, N. G., TARNEY, J. & HENDRY, G. L. (1983). Trace element geochemistry of basalts from Hole 504B, Panama Basin, DSDP Legs 69 and 70. *Init. Rept. Deep Sea Drilling Project. 69, 747-764*. (U.S. Govt. Printing Office, Washington).
- MIGOIS, G. (1983). *Geological study of the Kato Olympos area, Thessaly*. Ph.D. thesis, Patra, p.204.
- MOUNTRAKIS, D. (1983). *Structural geology of the North Pelagonian Zone s. l. and the geotectonic evolution of the Internal Hellenides*. Docent thesis, University of Thessaloniki, 289 pp.
- PEARCE, J. A., HARRIS, N.B.W. & TINDLE, A. J. (1984) Trace elements discrimination diagrams for the tectonic interpretation of the granitic rocks. *J. Petrol.*, 25, p.956-983
- SCHERMER, E. R., LUX, D. R. & BURCHFIEL, B. C. (1989). Age and tectonic significance of metamorphic events in the Mt. Olympos region, Greece. *Bul. Geol. Soc. Greece*, 23/1 p. 13-27.
- STAMATIS, A. (1987). *Geological map of Greece, (1:50000) Deskati sheet*, Publication IGME.
- TULLOCH, A.J. (1979). Secondary Ca-Al silicates as low-grade alteration products of granitoid biotite. *Contr. Min. Petr.*, 69, p. 105-117.
- WONES, D. R. & EUGSTER, H. P. (1965). Stability of biotite: experiment, theory and application. *Am. Min.*, 50, p. 1228 -1278.
- WOOD, D. A., JORON, J. L., TREUIL, M. & TARNEY, J. (1979). Elemental and Sr isotope variations in basic lavas from Iceland and the surrounding ocean floor. *Contrib. Min. Petr.*, 70, p. 319-339.